The effect of electronic disequilibrium on the received dose by lung in small fields with photon beams: Measurements and Monte Carlo study

A. Mesbahi*

Medical Physics Department, Medical School and Radiation Oncology Department, Imam Khomeini Hospital, Tabriz University of Medical Sciences, Tabriz, Iran

Background: Prediction of the absorbed dose in irradiated volume plays an important role in the outcome of radiotherapy. Application of small fields for radiotherapy of thorax makes the dose calculation process inaccurate due to the existence of electronic disequilibrium and intrinsic deficiencies in dose calculation algorithms. To study the lung absorbed dose in radiotherapy with small fields, the central axis absorbed dose in heterogeneous thorax phantom was measured by ionization chamber and calculated for small fields by Monte Carlo (MC) method. *Materials and Methods:* A solid slab phantom consisting of unit and low density materials was used for dose measurements. The 6 and 18 MV photon beams of Elekta SL25 linac were simulated using MCNP4C MC Code. The model was validated by comparing the calculated depth dose and beam profiles with measurements in a water phantom. The MC model was used to calculate the depth doses in unit density and low density materials resembling the soft tissue and lung, respectively. Two small field sizes including 5×5 and 2×2 cm² were used in this study. *Results:* The measured depth dose values were in good agreement with MC results and the difference less than 2% was observed. A large dose reduction was seen in lung for field size of 2×2 cm² due to the lateral electronic disequilibrium and it reached up to 16.2% and 33.3% for 6 and 18 MV beams, respectively. Dose build up and down at material interfaces was predicted by MC method. *Conclusion:* Our study showed that the dose reductions with small fields in lung and dose variations at interfaces was very considerable, and inaccurate prediction of absorbed dose in lung using small fields and photon beams may lead to critical consequences for patients. **Iran. J. Radiat. Res., 2008; 6 (2): 70-76**

Keywords: Electronic disequilibrium, radiotherapy of lung, Monte Carlo method.

INTRODUCTION

Application of small fields in radiotherapy is going to be a routine procedure in recent radiotherapy techniques such as three dimensional conformal radiotherapy, intensity modulated radiotherapy (IMRT) and linac-based radio-surgery [1-3]. The main problem with the small fields in high energy photon beams is the lateral electronic disequilibrium (LED) which makes the prediction of the delivered dose to the target volume unreliable [4-7]. Analytic dose calculation methods in most of commercial treatment planning systems (TPSs) have shown significant inaccuracy in calculations for small fields especially in low density media such as lung [5,8-10]. Fortunately, the Monte Carlo (MC) method has shown considerable accuracy in dose calculations for small fields in lung irradiations, where both lateral and forward electronic disequilibrium exists. Application of small fields in homogeneous unit-density media causes under dosage of target volume due to LED. On the other hand, the problem of LED becomes pronounced in low density media, due to the existence of fewer atoms along the pathway of photons, and it causes the lack of secondary electrons consequently. The other effect of LED in lung is the enlargement of beam penumbra which increases the under dosage of target volume at the edge of beam[11]. This problem could be very important for small fields where the coverage of target with the optimum isodose curve is necessary. Forward electronic disequilibrium (FED) occurs at

Corresponding author:
Dr. Asghar Mesbahi, Medical Physics Department, Medical School, Tabriz University of Medical Sciences, Tabriz, Iran.
Fax: +98 411 3364660
Email: asgharmesbahi@yahoo.com

the media interfaces with different material densities. Thus, the number of electrons generated in one side may be either more or less than the electrons generated on the other side [12]. The extent of FED has changed with density of materials at the interfaces and photon energies. However, this effect is prominent for higher photon energies and lung-soft tissue and air-soft tissue interfaces.

In the present study, the effect of LED and FED on the delivered dose in low density media are evaluated, resembling the lung tissue in the presence of small fields using ionization chamber measurements in slab phantom. Also, the geometry has been simulated using MCNP4C MC Code and the absorbed dose are calculated by the MC method.

MATERIALS AND METHODS

Inhomogeneous thorax phantom measurements

An inhomogeneous slab phantom consisting of polyethylene with density of 0.97 g/cm^3 and cork slabs with density of 0.2 g/cm^3 were used as a geometry resembling to the lateral irradiations of thorax (figure 1). For point dose measurement in slab phantom, a pinpoint chamber type 31006 with 0.015 cm^3 sensitive volume, and a Unidose E-electrometer of the PTW-Freiburgh were used. According to the manufacturer's recommendations, in order to get reliable results, the chamber was connected to the electrometer for 10 minutes and pre-irradiated with 2 Gy. Three readings were obtained and averaged for each point. The readings were corrected for temperature and pressure changes during the measurements. The reference points for the normalization of readings were points at the depths of 1.5 and 3 cm (depth of maximum dose) for 6 and 18 MV beams on the central axis of the beam, respectively. All irradiations were made at the source to surface distance

(SSD) of 100 cm. For the relative dose measurements in a thorax phantom, the uncertainty of measurements was ±1.5%. Relative readings of the chamber at each point to the reference point readings were multiplied by 100 and considered as percent depth dose for each point.
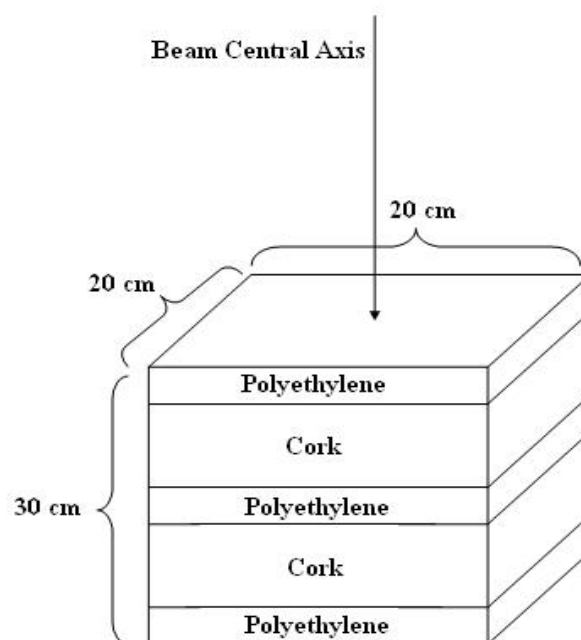

Figure 1. Sketch of solid slab phantom geometry used for measurement and MC simulations.

Monte Carlo modeling of Elekta SL 25 linac

The MCNP4C MC code is currently used to create and evaluate the phase space distributions from linear accelerator simulations[13]. This code allows for the development of detailed 3D models of a linear accelerator treatment head.

In the present study the head of Elekta SL-25 was completely simulated based on manufacturer's detailed information. The components of a linear accelerator for 6 and 18 MV photon beams are shown in figure 2. The model constructed to simulate the Elekta SL-25 linear accelerator radiation head incorporated the major components in the beam path. The target comprised of tungsten (95%), nickel
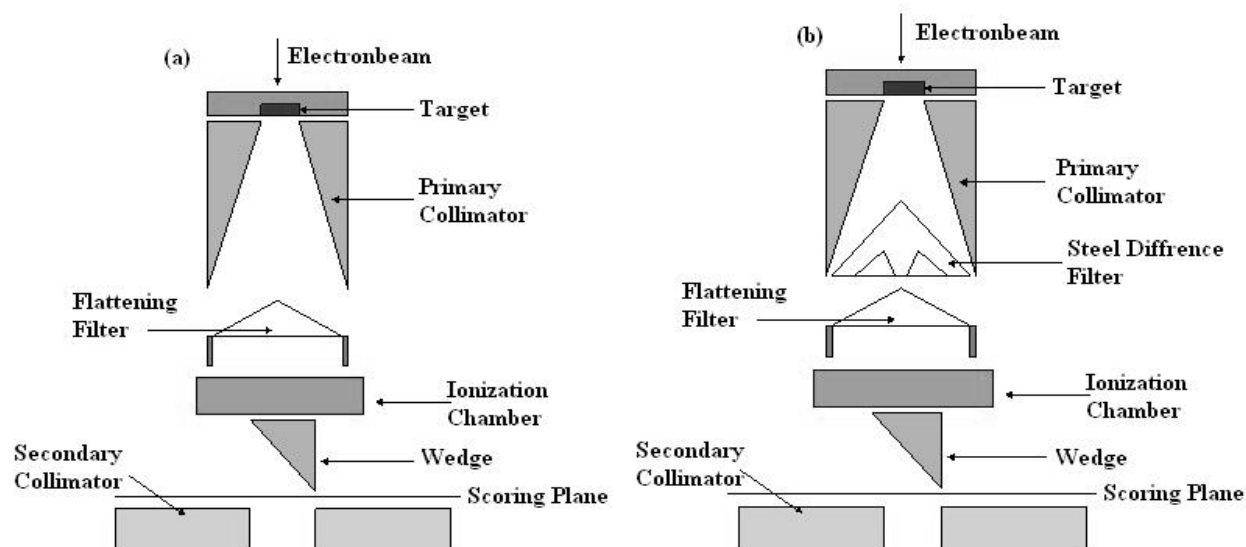
Figure 2. The schematic representation of Elekta 25 SL Linac head geometry used for simulation of (A) 6 MV and (B) 18 MV photon beams. In our simulation the ionization chamber and wedge were not included.

(3.75%) and iron (1.25%) alloy of density 18.0 g/cm³, attached to a copper backing plate. The incident electron beam striking the target was simulated by a spot size of 1 mm full width half maximum (FWHM) at the nominal accelerating potential of 6 and 18 MeV. Immediately under the target was the primary conical collimator comprising a 28° cone bored in a metal (lead 96% and antimony 4%, density 11.12 g/cm³) block. The flattening filter for each energy was simulated according to the detailed geometry drawings provided by manufacturer. For 18 MV beam a differential filter was added to 6 MV filters to create desired radiation intensity across the beam.

The Elekta SL-25 linear accelerator with a double plane adjustable diaphragm system providing secondary collimation has been the final component to be modeled. The collimating face of each diaphragm (composition: lead 96% and antimony 4%) moves in such a way that it always lies along the direction of propagation of the radiation, i.e. along a radius from the source.

A complete model of the linac was developed with the above mentioned components. Then, a water phantom with dimension of 50×50× 50 cm³ was simulated under treatment head with source-surface distance (SSD) of 100 cm, and the secon-

dary collimators was set to create a field size of 10×10 cm² on phantom surface.

The exact mean energy of the electron beam incident on target is typically unknown and must be obtained by calibrating each spectral distribution against the corresponding depth dose curve by a trial-and-error method by choosing a suitable mean electron energy exiting the flight tube. Primary electron beam energies of both photon beams were determined by calculation of percent depth doses (PDD) for different energies of primary electron beams. For both beams, the percentage depth doses (PDDs) for 10×10 cm² field size were calculated. The range of primary electron energy was 6-6.5 for 6 MV photons and 17.8-18.3 MeV for 18 MV. By comparing calculated PDD with measurements, the primary electron energy for 6 and 18 MV photons were determined to be 6.4 and 18, respectively.

The measured data were obtained by RFA 300 (Scanditronix) automatic water phantom. The PDDs for 2×2, 5×5, 10×10, 20×20 and 30 ×30 cm² field sizes and beam profiles for different field sizes at 10 cm depth were calculated using MC method and compared with the measurements. For depth dose calculations in water phantom, a cylinder with radius of one-tenth of the size of the open filed size was defined and

divided into scoring cells with 2 mm height along the beam central axis. The simulation setup for beam profile calculations was identical to the depth dose calculations, except for the primary cylinder which was located at 10 cm depth vertically to beam central axis. The radius of cylinder was 2 mm. The dose resolution for depth dose and beam profile was 2 mm.

The photon and electron low-energy cut-off was 10 and 500 keV respectively. The *F8 tally was used for dose calculations in water and thorax phantom. For all MC calculations the statistical uncertainty of results was less than 1% at d_{max}.

Water phantom benchmarks

Percentage depth dose curves for both energies and different field sizes were calculated and compared with the measurements. The PDD curves and beam profiles for both energies are shown in figures 3 and 4. In both figures, each beam profile was normalized to its maximum value in central axis and was scaled for inclusion on the same graph. All depth dose curves were normalized to d_{max} and were scaled for inclusion on the same graph. There was a good agreement for MC calculations versus the measurements in all parts of the depth dose curve including the build-up region. The difference between measurements and MC calculations was less than 1.5% for descending part of PDD curves for both energies. But, however, for build-up region, it reached up to 15% near the surface of phantom for 30×30 cm² field sizes in 18 MV beam.

Beam profiles for the different field sizes at the depth of 10 cm were calculated and compared by the measurements. Figures 3-A and 4-A illustrate the comparison between MCNP4C profile calculations and water phantom measurements for both beam energies. For points within the 50%-100% isodose range the differences up to 3% were observed. The great local difference in this region also was reported

by other previous investigations [10, 14, 15]. However, this difference was at out of field region, which was delivered by the scattered radiations and does not affect the results in central axis of the beam. Also, according to recommended criteria for this region if the differences were normalized to maximum value in beam profiles, the differences would have been within acceptable value of 3% [16].

RESULTS

Absorbed doses in inhomogeneous solid phantom

The central axis absorbed doses in irradiated phantom are shown in figures 5 and 6. The MC results are in close agreement with measurements for both
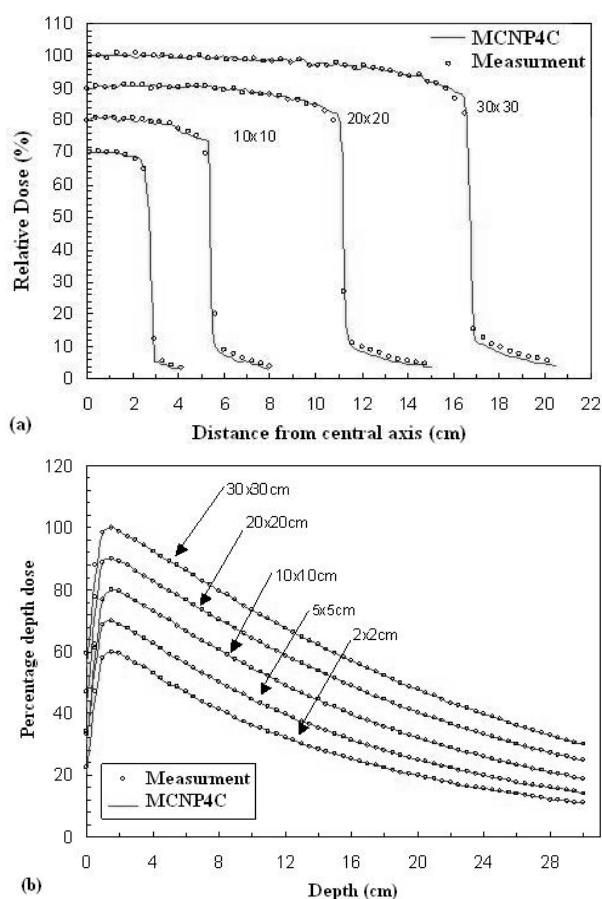

Figure 3. (A) Comparison of the MC beam profile calculations versus water phantom measurements for 6 MV photon beam at 10 cm depth. (B) Comparison of MC depth dose calculations versus water phantom measurements for 6 MV photon beam.
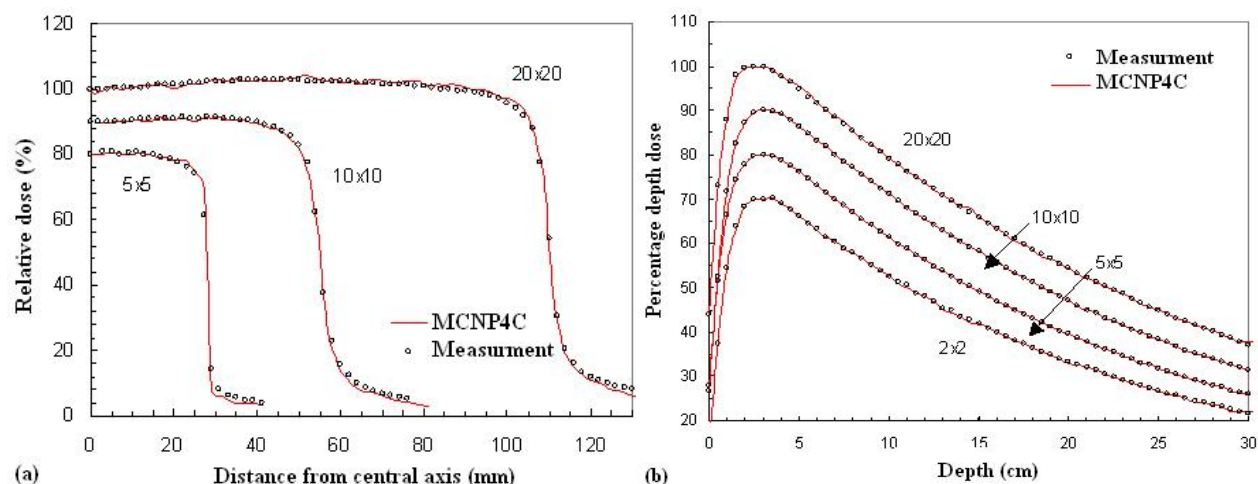
Figure 4. (A) Comparison of the MC profile calculations versus water phantom measurements for 18 MV photon beam at 10 cm depth. (B) Comparison of MC depth dose calculations versus water phantom measurements for 18 MV photon beam.

field sizes and energies (difference less than 2%). It can be seen that the absorbed depth dose is reduced significantly in low density medium for both field sizes and energies. The dose reduction in low density was very pronounced for 2×2 cm² field size, because in this field size LED exists for both unit and low density media. For 6 MV beam, the amount of dose reduction in lung in comparison with the absorbed dose values had reached in water phantom for the same field size to the maximum of 16.2%, while it was 1.4% for the field size of 5×5 cm². The dose reduction in the second low density material was lower than that of the first for both field sizes; because, in the deeper region of the phantom, the contribution of scattered radiation in absorbed dose had increased and it slightly compensated the effect of LED in the   second low density material.

For the 18 MV beam, due to the higher range of secondary electrons, the LED became more prominent. For 2× 2 cm² field size, there was sharp fall-off in the absorbed dose of low density material, especially for the first low density material in the pathway of the high energy photons. The amount of dose reduction was about 33.3% for the point in the middle of first low density material. By increasing the field size to 5×5 cm² the value was decreased and became 7.7%. Although the
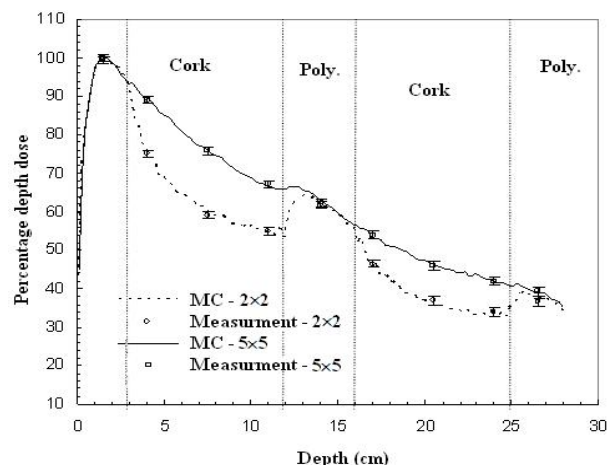

Figure 5. Comparison of MC calculated depth doses and ionization chamber measurements for the 6 MV photon beam.
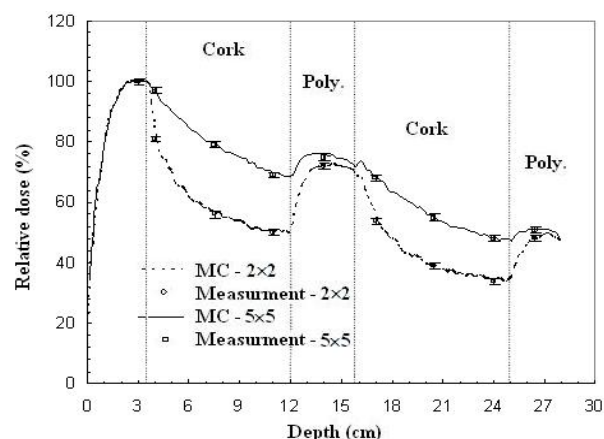

Figure 6. Comparison of MC calculated depth doses and ionization chamber measurements for the 18 MV photon beam.

dose reduction in low density medium for both energies are predictable for field size of 5×5 cm², the dose reduction of 16% and

33% for 6 and 18 MV beams showed that the dosimetric consequences of LED in lung to be highly considerable. The erroneous calculations in low density inhomogeneities such as lung could have led to under dosage of target volume and fatal outcomes for patients. MC code predicted the effect of LED, due to electron transport modeling in the MC code of MCNP4C. Several studies on the TPSs have showed that they were not capable to model the secondary electrons especially in inhomogeneities existing in the patients body [9,17,18]. Of course, the calculations in small field sizes were inaccurate enough to exclude them form dose calculations in treatments involving small fields such as IMRT, and three dimensional conformal radiotherapy. In a study by Mesbahi *et al.* on the Eclipse TPS for 8 and 15 MV photon beams, a considerable dose reduction in low density material was seen for 4×4 cm^2 field size. The results showed the errors of up to 33% and 28% in the lung (for 15 MV beam) for TPS calculations using Modified Batho and equivalent tissue-air ratio methods respectively [9].

In a recent study on the accuracy of lung dose calculations by Collapsed Cone Convolution (CCC), Batho, and Monte Carlo methods, they showed that the CCC and MC methods had better performance and were sensitive to the absorbed dose changes due to electronic disequilibrium at interfaces and lateral electronic disequilib-rium in the lung for small fields [19]. FED is another concern at the interfaces. In the current study, there were unit density and lung tissue-like interfaces. In figures 5 and 6, two regions are apparently shown as the polyethylene-cork (P-C) and cork-poly ethylene (C-P) interfaces. In P-C interface, the absorbed dose had reduced abruptly due the loss of secondary electrons in the cork and the dose build down region was created. However, in C-P interface the dose build up region was generated due to more secondary electrons production in unit

density medium; and, at a short distance, the forward electronic equilibrium was created. The interface effect was very pronounced for 18 MV photon beam, since the range of secondary electrons was longer, and it needed more length for them to make the electronic equilibrium. The technical difficulties associated with experimental measurement of interface effect, made MC method a reasonable way to study the FED in interfaces.

MC results of the present study showed differences less than 2% in comparison with the measurements. Also, MC method showed LED and FED condition at inhomogeneous solid phantom. The results were in accordance with those the results of the previous studies on the small field sizes used in IMRT [2, 4, 6, 7, 19, 20]. The study of Jones and Das shows that for a 6 MV photon beam, electronic equilibrium was restored at field sizes above 3 cm diameter and all of the algorithms predict dose in and beyond the inhomogeneous region equally well [21]. In the present study the difference between water phantom and lung dose values in a 5×5 cm^2 field size were 1.4% indicating the existence of electron equilibrium for the field size. The existence of FED and consequently the build down and build up regions at tissue interfaces, might have caused under or overdosage of target volume situated in these regions. On the other hand, accurate prediction absorbed in interfaces was difficult with current TPSs. Therefore, the application of MC method or other algorithms, capable to account for LED and FED are necessary in treatments with small fields and high energy photons.

CONCLUSION

The LED and FED effects were studied using an inhomogeneous solid phantom resembling the thorax region. The absorbed dose on beam central axis in unit density and low density materials was

measured and calculated using MC method. The finding showed that the absorbed in lung tissue was decreased significantly in a small field of 2×2 cm² where LED did not exist. The prediction of the absorbed dose in small field needed algorithms which modeled the transport of secondary electrons in the irradiated medium. MCNP4C MC Code was capable to calculate the dose in the regions with FED and LED conditions.

REFERENCES

1. Brugmans MJ, van der HA, Lebesque JV, Mijnheer BJ (1999) Beam intensity modulation to reduce the field sizes for conformal irradiation of lung tumors: A dosimetric study. *Int J Radiat Oncol Biol Phys,* **43:** *893-904.*
2. Calcina CS, de Oliveira LN, de Almeida CE, de AA (2007) Dosimetric parameters for small field sizes using Fricke xylenol gel, thermoluminescent and film dosimeters, and an ionization chamber. *Phys Med Biol,* **52:***1431-1439.*
3. De JK, Hoogeman MS, Engelsman M, Seppenwoolde Y, Damen EM, Mijnheer BJ, Boersma LJ, Lebesque JV (2003) Incorporating an improved dose-calculation algorithm in conformal radiotherapy of lung cancer: re-evaluation of dose in normal lung tissue. *Radiother Oncol,* **69:** *1-10.*
4. Cheng CW, Das IJ, Huq MS (2003) Lateral loss and dose discrepancies of multileaf collimator segments in intensity modulated radiation therapy. *Med Phys,* **30:** *2959-2968.*
5. Farajollahi A and Mesbahi A (2006) Monte Carlo dose calculations for a 6-MV photon beam in a thorax phantom. *Radiat Med,* **24:** *269-276.*
6. Francescon P, Cora S, Chiovati P (2003) Dose verification of an IMRT treatment planning system with the BEAM EGS4-based Monte Carlo code. *Med Phys,* **30:** *144-157.*
7. Fu W, Dai J, Hu Y (2004) The influence of lateral electronic disequilibrium on the radiation treatment planning for lung cancer irradiation. *Biomed Mater Eng,* **14:** *123-126.*
8. Mesbahi A, Allahverdi M, Gheraati H (2005) Monte Carlo dose calculations in conventional thorax fields for 60Co photons. *Radiat Med,* **23:** *341-350.*
9. Mesbahi A, Thwaites D, Reilly A (2006) Experimental and Monte Carlo evaluation of Eclipse treatment planning system for lung dose calculations. *Rep Pract Oncol Radiother,* **3:** *1-11.*
10. Miften M, Wiesmeyer M, Kapur A, Ma CM (2001) Comparison of RTP dose distributions in heterogeneous phantoms with the BEAM Monte Carlo simulation system. *J Appl Clin Med Phys,* **2:** *21-31.*
11. Tsiakalos MF, Theodorou K, Kappas C, Zefkili S, Rosenwold JC (2004) Analysis of the penumbra enlargement in lung versus the quality index of photon beams: a methodology to check the dose calculation algorithm. *Med Phys,* **31:** *943-949.*
12. Woo MK, Cunningham JR, Jezioranski JJ (1990) Extending the concept of primary and scatter separation to the condition of electronic disequilibrium. *Med Phys,* **17:** *588-595.*
13. Briesmeister JF (2000) MCNP-A general Monte Carlo N-particle transport code, Version 4C. Report LA-13709-M. Los Alamos National Laboratory, NM.
14. Mesbahi A, Fix M, Allahverdi M, Grein E, Garaati H (2005) Monte Carlo calculation of Varian 2300C/D Linac photon beam characteristics: A comparison between MCNP4C, GEANT3 and measurements. *Appl Radiat Isot,* **62:** *469-477.*
15. Mesbahi A, Reilly AJ, Thwaites DI (2006) Development and commissioning of a Monte Carlo photon beam model for Varian Clinac 2100EX linear accelerator. *Appl Radiat Isot,* **64:** *656-662.*
16. Venselaar J, Welleweerd H, Mijnheer B (2001) Tolerances for the accuracy of photon beam dose calculations of treatment planning systems. *Radiother Oncol,* **60:** *191-201.*
17. Kan MW, Wong TP, Young EC, Chan CL, Yu PK (1995) A comparison of two photon planning algorithms for 8 MV and 25 MV X-ray beams in lung, Australas. *Phys Eng Sci Med,* **18:** *95-103.*
18. Vanderstraeten B, Reynaert N Paelinck L, Madani I, De WC, De GW, De NW, Thierens H (2006) Accuracy of patient dose calculation for lung IMRT: A comparison of Monte Carlo, convolution/superposition, and pencil beam computations. *Med Phys,* **33:** *3149-3158.*
19. Arnfield MR, Siantar CH, Siebers J, Garmon P, Cox L, Mohan R (2000) The impact of electron transport on the accuracy of computed dose. *Med Phys,* **27:** *1266-1274.*
20. Chetty I, Moran JM, Nurushev TS, McShan DL, Fraass BA, Wilderman SJ, Bielajew AF (2002) Experimental validation of the DPM Monte Carlo code using minimally scattered electron beams in heterogeneous media. *Phys Med Biol,* **47:** *1837-1851.*
21. Jones AO and Das IJ (2005) Comparison of inhomogeneity correction algorithms in small photon fields. *Med Phys,* **32:** *766-776.*